Plasmonic Phase-Gradient Image Sensors

Jianing Liu, Yuyu Li, Hao Wang, Lei Tian, and Roberto Paiella

Department of Electrical and Computer Engineering and Photonics Center, Boston University, 8 St. Mary's St., Boston, MA 02215, USA Email address: ljn@bu.edu

Abstract: We report plasmonic metasurface photodetectors featuring a strong asymmetric angular response around normal incidence that can visualize transparent phase objects with high sensitivity in a simple and compact imaging setup. © 2022 The Author(s)

1. Introduction

Traditional image sensors can only capture the intensity distribution of the incident light, whereas all information associated with the phase profile is lost in the image acquisition process. Therefore, these devices cannot directly visualize transparent phase objects, as required for applications such as label-free microscopy of biological samples [1] and surface profiling (e.g., for semiconductor chip inspection). Transmission or reflection of light from phase-only objects generally involves a deflection $\Delta\theta$ in the direction of light propagation proportional to the local phase gradient $\nabla \phi$ [Fig. 1(a)]. As a result, the visualization of such objects requires an imaging system whose response varies with illumination angle around normal incidence. Various systems have already been developed for this purpose [1], but normally involve rather complex and bulky setups that limit their range of applications.

Here we describe angle-sensitive image sensors that can measure the phase gradient of the incident optical field directly, without the need for any external optical elements other than standard imaging lenses. These devices consist of photodetectors stacked with a composite plasmonic metasurface designed to introduce a strong dependence of responsivity $\mathcal R$ on illumination angle θ [Figs. 1(b)-(d)]. Similar devices, with responsivity peaked at geometrically tunable angles across an ultrawide field of view of 150°, were developed in prior work to demonstrate flat lensless compound-eye vision [2]. A variation of the same approach, with metasurfaces producing a symmetric response $\mathcal R(\theta)$ about normal incidence, has also been used to perform various optical-spatial-filtering operations [3].

In the present work, we report a new device structure featuring an asymmetric response $\mathcal{R}(\theta)$ with a sharp peak centered at a small illumination angle $\theta \approx 2^{\circ}$, such that the low-angle tail of the peak overlaps with normal incidence [Fig. 1(d)]. This design allows maximizing the responsivity slope $d\mathcal{R}/d\theta$ near $\theta=0$. As a result, if an array of these devices is used to visualize a transparent phase object, even a small phase gradient $\nabla \phi$ in the object (i.e., a small deflection angle $\Delta \theta$ in the transmitted or reflected light) can produce a detectable contrast in the image captured by the array. To quantify the resulting imaging performance, we have used the measured angle-dependent characteristics of an experimental sample to evaluate the minimum detectable phase contrast. A value as small as $0.003 \times 2\pi$ is obtained, highlighting the promise of these devices to dramatically simplify and miniaturize phase-imaging systems while still providing state-of-the-art sensitivity.

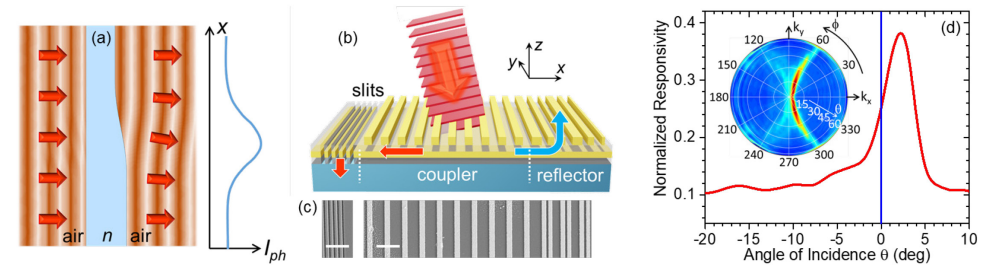


Fig. 1. (a) Schematic illustration of light transmission through a phase object and its detection with an angle-sensitive photodetector. (b) Device structure developed in this work. (c) Top-view SEM images of an experimental sample. The scale bars are 2 μm. (d) Inset: measured responsivity vs polar and azimuthal angles of incidence for p-polarized light at 1550 nm. Main plot: horizontal line cut of the color map. The peak responsivity is normalized to that of an identical device without any metasurface. The vertical blue line indicates normal incidence.

2. Results and discussion

In the device architecture of Fig. 1(b), the illumination window of a photodetector is coated with a $SiO_2/Au/SiO_2$ stack. A periodic array of Au nanostripes (grating coupler) is then introduced over the top SiO_2 layer, surrounded on one side by a set of subwavelength slits perforated through the stack and on the other side by an aperiodic section of Au nanostripes of different widths (reflector). The Au film is sufficiently thick (100 nm) to block any incident light from being transmitted directly into the device active layer. Therefore, photodetection can only take place through a

plasmon-assisted process where light incident at the target detection angle $+\theta_p$ is first diffracted by the grating coupler into surface plasmon polaritons (SPPs) on the top surface of the Au film. These SPPs eventually reach the slit section, where they are preferentially scattered into the underlying photodetector active layer (similar to the phenomenon of extraordinary optical transmission). Light incident at the opposite angle $-\theta_p$ is diffracted by the grating coupler into SPPs propagating towards the reflector, which is designed (based on the notion of gap-plasmon metasurfaces) to scatter the incoming SPPs back into the air above. The desired asymmetric angular response is thus enabled by this diverging action of the slits and reflector on oppositely traveling SPPs. Finally, light incident along any other direction is simply reflected or diffracted directly into radiation propagating away from the device surface.

For convenience, the specific devices developed in this work are based on simple Ge photoconductors operating at 1550-nm wavelength, although the same metasurface of Fig. 1(b) could be applied to many other types of image sensors. The measured response map (responsivity \mathcal{R} versus polar θ and azimuthal ϕ illumination angles) displays the expected angular selectivity [inset of Fig. 1(d)]. Specifically, the incident directions of high responsivity form a rather narrow region within the full hemisphere, with a distinctive curved shape determined by diffraction of the incoming light into different SPP modes. The horizontal line cut of the color map, shown in the main plot of Fig. 1(d), features the expected peak immediately adjacent to normal incidence with large linear slope $d\mathcal{R}/d\theta$ at $\theta=0$. The responsivity at the angle of peak detection $\theta_p\approx 2^\circ$ is about 38% of that of an identical uncoated device, indicating that the metasurface transmission penalty is reasonably small.

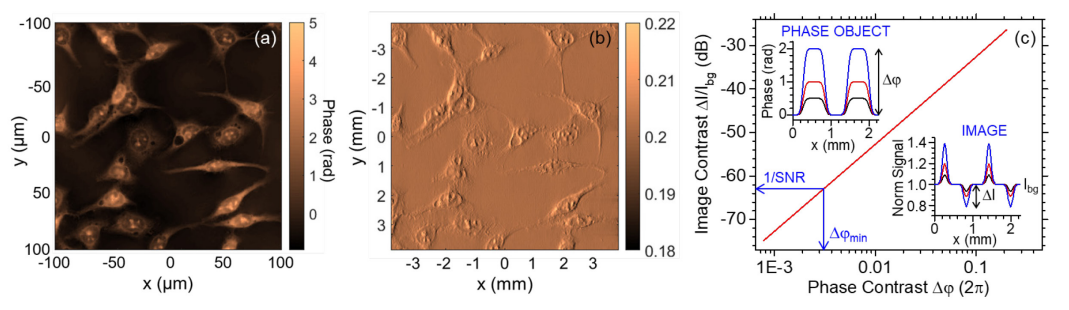


Fig. 2. Phase imaging results. (a) Object (HeLa cancer cells). (b) Corresponding image. (c) Relative image contrast $\Delta I/I_{bg}$ vs object phase contrast $\Delta \phi$ for a 1D phase grating (upper inset) producing the image shown in the lower inset.

Next, we evaluate the phase contrast imaging capabilities of an image sensor array based on the devices just described. As an example of a phase object of practical interest, we consider the transparent biological sample shown in Fig. 2(a) (HeLa cancer cells). Figure 2(b) shows the image of this object computed from the experimental data of Fig. 1(d)-inset with a frequency-domain approach, for a 357×357 pixel array combined with a 40× magnification imaging system. Despite being fully transparent, the individual cells are well resolved in the image, as a result of the strong angular sensitivity of these devices.

For a more quantitative evaluation, Fig. 2(c) shows results obtained with another object – a 1D phase grating of variable phase contrast $\Delta \varphi$ (upper inset). From the resulting image (lower inset), we can quantify the image contrast ΔI and background signal I_{bg} . The red line in Fig. 2(c) shows the ratio $\Delta I/I_{bg}$ versus $\Delta \varphi$. The phase object can be detected as long as $\Delta I/I_{bg} > 1/\text{SNR}(I_{bg})$, where $\text{SNR}(I_{bg})$ is the device signal-to-noise ratio at the background signal level. The latter quantity can be evaluated based on the reported SNR values for near-infrared photodetectors of comparable dimensions as the present devices [horizontal arrow in Fig 2(c)] [4]. Correspondingly, a minimum detectable phase contrast $\Delta \varphi_{min}$ of $0.003 \times 2\pi$ is estimated [vertical arrow], within the same order of magnitude of state-of-the-art phase imaging systems involving significantly more complex and bulky setups [5].

This work was supported by NSF under Grant ECCS 2139451.

3. References

- [1] T. L. Nguyen, S. Pradeep, R. L. Judson-Torres, J. Reed, M. A. Teitell, and T. A. Zangle, "Quantitative phase imaging: recent advances and expanding potential in biomedicine," ACS Nano 16, 11516-11544 (2022).
- [2] L. Kogos, Y. Li, J. Liu, Y. Li, L. Tian, and R. Paiella, "Plasmonic ommatidia for lensless compound-eye vision," Nat. Commun. 11, 1637 (2020).
- [3] J. Liu, H. Wang, L. C. Kogos, Y. Li, Y. Li, L. Tian, and R. Paiella, "Optical spatial filtering with plasmonic directional image sensors," Opt. Express 30, 29074–29087 (2022).
- [4] M. Murata et al., "A high near-infrared sensitivity over 70-dB SNR CMOS image sensor with lateral overflow integration trench capacitor," IEEE Trans. Electron Devices 67, 1653-1659 (2020).
- [5] C. Bonati, T. Laforest, M. Kunzi, and C. Moser, "Phase sensitivity in differential phase contrast microscopy: limits and strategies to improve it," Opt. Express 28, 33767-33783 (2020).